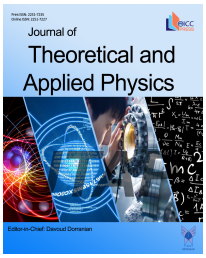

Volume 18, Issue 1, 182413 (1-7)

Journal of Theoretical and Applied Physics (JTAP)

https://dx.doi.org/10.57647/j.jtap.2024.1801.13

Chromium ions effects on Sb_2O_3-PbO-GeO_2 glass properties for radiation protection

Mohammed I. Sayyed[1,2], Kawa M. Kaky[3]*, Rana A. Anaee[4]

[1]*Department of Physics, Faculty of Science, Isra University, Amman, Jordan.*
[2]*Department of Nuclear Medicine Research, Institute for Research and Medical Consultations, Imam Abdulrahman Bin Faisal University, Dammam, Saudi Arabia.*
[3]*Al-Nisour University College, Baghdad, Iraq.*
[4]*Department of Materials Engineering, University of Technology, Baghdad, Iraq.*

***Corresponding author:** kawa.mudher@gmail.com

Original Research

Received:
10 July 2023
Revised:
1 September 2023
Accepted:
9 September 2023
Published online:
10 January 2024

Abstract:

In this work we studied the radiation shielding features of Li_2O-Sb_2O_3-PbO-GeO_2-Cr_2O_3 glass systems at different energies ranging from 0.284 to 1.33 MeV. The maximum linear attenuation coefficient (LAC) for the germinate glasses is in the order of 0.680-0.707 cm^{-1} and this is reported at 0.284 MeV, whereas the minimum LAC is observed at 1.33 MeV and varied between 0.159-0.166 cm^{-1}. An increase in the LAC is found for these glasses due to the addition of Cr_2O_3, and the glasses coded as C5 (with 0.5 mol% of Cr_2O_3) has the highest LAC. The half value layer (HVL) of the selected glasses with different contents of Cr_2O_3 is investigated, and the results demonstrated that the HVL is small at low energies and ranging from 0.98-1.02 cm at 0.284 MeV and from 1.328-1.383 cm at 0.347 MeV. The maximum HVL is observed at 1.33 MeV and equal to 4.175 cm for C5 and 4.352 cm for C1. The tenth value layer (TVL) values for the present glasses were reported, and the results showed that as the density increases from 3.07 to 3.2 g/cm^3, the TVL decreases from 3.388 to 3.256 cm at 0.284 MeV, and from 13.413 to 12.868 cm at 1.173 MeV.

Keywords: Photon radiation shielding; Half value layer; Lead glasses; Germanate glasses; Effective atomic number; Attenuation

1. Introduction

Ionizing radiation has become an indispensable instrument in the field of medicine, serving both diagnostic and therapeutic purposes for a diverse array of medical conditions [1–3]. The cumulative radiation exposure experienced by both patients and medical practitioners has undergone modifications in tandem with its utilization [4–6]. Proficiency in comprehending the hazards of radiation exposure and implementing techniques to mitigate radiation dose will be imperative as the prevalence of radiation on exposure continues to rise [7, 8]. In order to eliminate or reduce the level the radiation in the place of work for the safety of worker many research started to work on this field for decades [9]. One of the standard and traditional protection materials is concrete, however it presents excellent absorption of radiation, but have in the other sides danger draw-back such as changing the eternal concrete structure by the time and appearing cracks that allow radiations to pass, moreover the concrete is non-visible material that make operator difficult to observe and supervise the station, impossible to maintain and move [10, 11]. From all these disadvantages we can conclude that concrete can be use in the main structure as outside roof, and walls [12]. Polymers is not effective to absorb radiation beside it has low working temperature range and non-visible [13]. Lead plate is used widely in the area around the radiation source, but it's also as mentioned martials very difficult to move and maintain beside its toxicity [14]. Glasses is gained alternative attention from researchers in many fields [15], such as: optical communication [16], optical wave guide [17], laser [18], solar panels [19] and uncountable applications due its transparency, wide temperature range, excellent mechanical features, durability, structure stability, and wide of composition range based on the desired application [20]. Glass

Table 1. The chosen Li_2O-Sb_2O_3-PbO-GeO_2-Cr_2O_3 glass samples and density.

Glass code	Glass composition	Density (gm/cm^3)
C1	$10Li_2O$-$29.9Sb_2O_3$-20PbO-$40GeO_2$-$0.1Cr_2O_3$	3.07
C2	$10Li_2O$-$29.8Sb_2O_3$-20PbO-$40GeO_2$-$0.2Cr_2O_3$	3.15
C3	$10Li_2O$-$29.7Sb_2O_3$-20PbO-$40GeO_2$-$0.3Cr_2O_3$	3.16
C4	$10Li_2O$-$29.6Sb_2O_3$-20PbO-$40GeO_2$-$0.4Cr_2O_3$	3.18
C5	$10Li_2O$-$29.5Sb_2O_3$-20PbO-$40GeO_2$-$0.5Cr_2O_3$	3.20

composition structure mainly depends on the glass former which is the main network of the glass itself. TeO_2, GeO_2, PbO, SiO_2, and B_2O_3 are common glass former [21]. In radiation protection application both density and transparency are very important roles [22]. In this work we studied the radiation shielding parameters of Li_2O-Sb_2O_3-PbO-GeO_2-Cr_2O_3 glass systems [23] at different energies ranging from 0.284 to 1.33 MeV. We investigated the impact of Cr_2O_3 on the radiation shielding parameters.

2. Theoretical principles

In this work we studied the radiation features of a previous $10Li_2O$-$(30-X)Sb_2O_2$-20PbO-$40GeO_2$-XCr_2O_3 glass system were X= 0.1, 0.2, 0.3, 0.4, and 0.5 as it presented in Table. 1 along with related densities.

The exponential attenuation rule is used to define the linear attenuation coefficient (μ) of any glass system [24]:

$$\mu = -\frac{\ln(I/I_0)}{x} \tag{1}$$

The intensity of initial photons is denoted by I_0, while the intensity of transmitted photons is denoted by I. The thickness of the medium is represented by x, measured in centimeters. The mass attenuation coefficient, also known as μ_m or MAC, is a fundamental parameter frequently utilized to assess the effectiveness of glass samples are used. The measurement concerns the probability of interaction between gamma photons and the glass sample, which could entail either scattering or absorption. The Multi-Angular Collimator (MAC) has the capability to evaluate a range of parameters, such as the effective atomic number (AN), electronic cross section, and half value layer, among others. The mass attenuation coefficient (μ_m) for a compound or mixture can be mathematically defined using the following equation [25]:

$$\mu_m = \frac{\mu}{\rho} = \Sigma_i w_i (\frac{\mu}{\rho})_i \tag{2}$$

The equation is expressed as follows: $(\mu/\rho)_i$ and w_i denote the mass attenuation coefficient and weight fraction of the ith component of the composition, accordingly the determination of the μ_m value for glass systems within a particular energy range can be achieved through the utilization of WinXCom software, which relies on the combination rule.

By utilizing the aforementioned fundamental parameter, numerous quantities can be derived, including but not limited to the total atomic as well as electronic cross-section, the effective atomic number, and the electron density. The determination of the overall atomic cross section (σ_a) is able to be achieved through the following method [26]:

$$\sigma_a = \frac{(\mu_m)_{glass}}{N_A \Sigma_i (w_i/A_i)} \tag{3}$$

The expression N_A" denotes the Avogadro constant, while "A_i" represents the atomic weight for the i^{th} component of the glass system. The unit of measurement utilized is in square centimeters per atom which can be expressed as below [27]:

$$\sigma_e = \frac{1}{N} \Sigma_i w_i \frac{f_i A_i}{z_i} \tag{4}$$

The variables z_i and f_i denote the atomic number and a fraction quantity of the i-th element, respectively. Unit of measurement is square centimeters per electron.

The dimensionless quantity known as z_{eff} can be derived from the values of σ_a and σ_e through the following equation [28–32]:

$$z_{eff} = \frac{\sigma_a}{\sigma_e} \tag{5}$$

Half Value Layer (HVL) is a parameter that characterizes the thickness of a material at which the intensity of gamma radiation transmitted through it is reduced to half of the incident intensity. The HVL is determined by the value of the linear attenuation coefficient (μ) as below [24]:

$$HVL = \frac{\ln 2}{\mu} \tag{6}$$

The concept of mean free path (MFP) pertains to the average distance that a photon can traverse prior to undergoing interaction with the absorber. The value of μ has been estimated as follows [25]:

$$MFP = \frac{1}{\mu} \tag{7}$$

3. Results and Discussion

Fig.1 exhibits the linear attenuation coefficient (LAC) for the five germinate glasses with different contents of Cr_2O_3. At lower energies, the LAC values for the glasses are high, but when the energy increases, we observed a decrease in the LAC. This suggests that radiation with low energies is likely to interact with the atoms of the glasses, so more attenuation is occurred. The maximum LAC is in the order of 0.680-0.707 cm^{-1} and this is reported at 0.284 MeV,

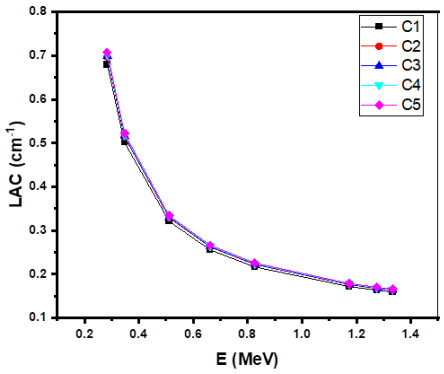

Figure 1. The linear attenuation coefficient for the five investigated germinate glasses.

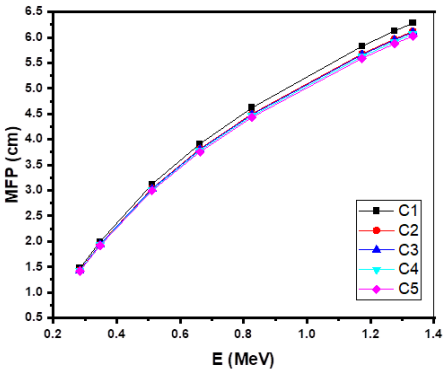

Figure 3. The mean free path for the five investigated germinate glasses.

whereas the minimum LAC is observed at 1.33 MeV and varied between 0.159-0.166 cm^{-1}. On the other hand, an increase in the LAC can be observed for these glasses due to the addition of Cr_2O_3. This is due to the fact that Cr_2O_3 has a density of 5.22 g/cm^3, so as we increase the content of Cr_2O_3, the density of the glasses is increased, which causes an increase in the LAC [26]. We found from Fig. 1 that C5 sample (with 0.5% mol of Cr_2O_3) has the highest LAC, while the glass with only 0.1 mol% of Cr_2O_3 is the sample with lowest LAC. Also, due to the Compton scattering process, we can see that the difference in the LAC values between the different glasses is very small. For example, the difference in the LAC between C1 and C5 glasses at 1.33 MeV is only 0.007.

The half value layer (HVL) of the C1-C5 glasses with different contents of Cr_2O_3 is investigated in Fig.2. The HVL of the glasses is small at low energies and ranging from 0.98-1.02 cm at 0.284 MeV and from 1.328-1.383 cm at 0.347 MeV. Hence, a small thickness of the glass is needed to attenuate the low energy radiation. On the other word, a sample of thickness of around 1-1.3 cm can be successfully absorb 50% of the incoming radiation with energy of 0.284-0.347 MeV. But we need a glass of thickness of about 2 cm to absorb 50% of the intensity the radiation with energy of 0.511 MeV, since the HVL at this energy is in the range of 2.076-2.162 cm. At higher energies, we found an increase in the HVL, where the HVL at 0.826 MeV is in the range of 3.072-3.201 cm [25–27]. The maximum HVL can be observed at 1.33 MeV and equal to 4.175 cm for C5 and 4.352 cm for C1. Contrary to what we found in Fig.1, adding Cr2O3 to the samples leads to a decrease in HVL. This is due to the inverse relation between the HVL and the LAC according to the basic formula HVL=0.693/LAC. So, we can easily see from Fig.2 that C5 glass has the smallest HVL.

The mean free path (MFP) for the C1-C5 samples with some energy values varying from 0.284 to 1.333 MeV is exhibited in Fig.3. Since C5 sample has the highest density among our selected glasses, the space between the atoms in this glass is the closest. Accordingly, C5 possesses the most interactions with the photons and as a result the smallest MFP, and this is clearly seen in Fig.3. In practical applications, the optimum glass for shielding the radiation is the sample with short MFP. So, we can conclude form this figure that adding more Cr_2O_3 to the glasses causes an increase in the density and thus reduce the MFP [33].

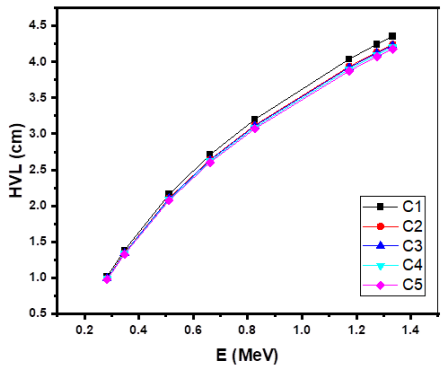

Figure 2. The half value layer for the five investigated germinate glasses.

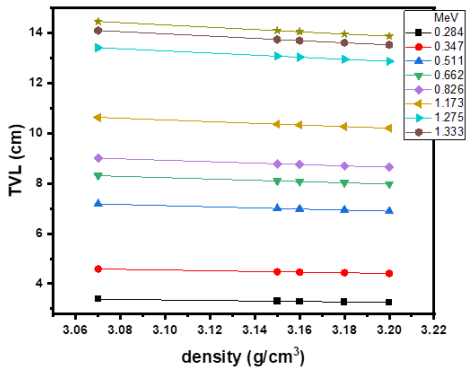

Figure 4. The tenth value layer for the five investigated germinate glasses.

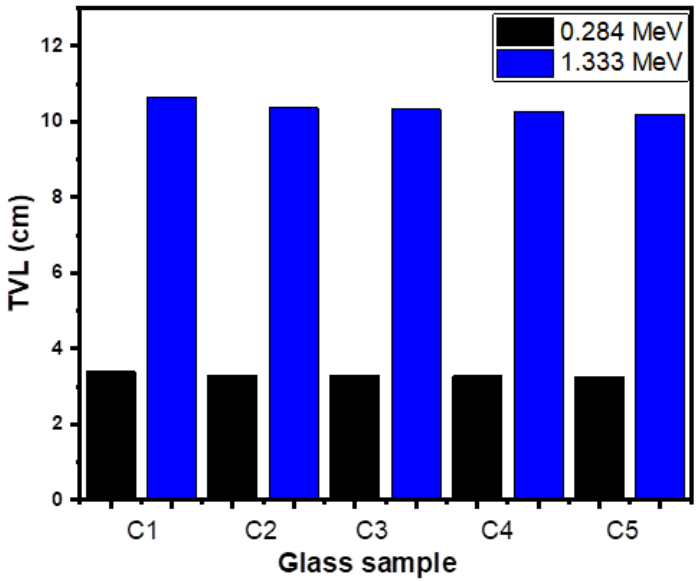

Figure 5. The TVL for each glass at both energies; 0.284 and 1.173 MeV.

Numerically, the MFP decreases from 1.995 to 1.916 cm at 0.347 MeV due to the addition of Cr_2O_3, while it decreases from 3.119 to 2.995 cm at 0.511 MeV. When we examined the relation between the MFP and the energy, we noticed that the MFP increases as the energy increases from 0.284 to 1.333 MeV. For example, for C1, we found that the MFP increases from 1.471 to 6.279 cm, while the MFP for C2 increases from 1.414 to 6.024 cm. This is in agreement with the HVL, since thicker material is required to attenuate the high energy radiation.

In Fig. 4, we investigated the relation between the tenth value layer (TVL) and the density of the glasses. It is easy to observe an inverse relation between the density and the TVL. As the density increases from 3.07 to 3.2 g/cm^3, the TVL decreases from 3.388 to 3.256 cm at 0.284 MeV, from 7.183 to 6.896 cm at 0.511 MeV and from 13.413 to 12.868 cm at 1.173 MeV. This indicates that the impact of high energy radiation can be minimized by increasing the density of the glass sample [34]. As a result, it is preferable to use HMO with appropriate concentrations in order to get high density shielding materials with superior shielding effectiveness.

Fig. 5 presents the TVL for each glass at both energies; 0.284 and 1.173 MeV. The aim of this figure is to examine the impact of the energy on the thickness of the glasses need to shield the incoming radiation. Apparently, for each glass, the TVL at 1.173 MeV is much higher than the TVL at 0.284 MeV. At 0.284 MeV, the TVL is in order of 3.25 cm, while this value is increased to 12.8-13.4 cm. This suggests that the thickness increases by a factor of about 4 when the energy increases from 0.284 and 1.173 MeV. When the low energy radiation enters the glass, many

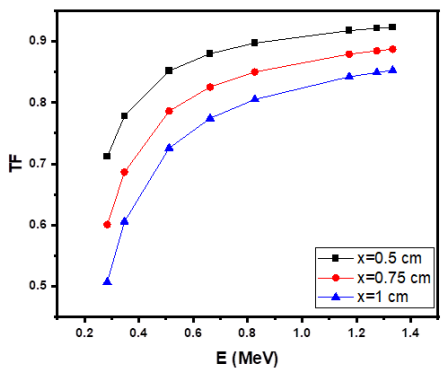

Figure 6. The transmission factor for C1 as a function of the energy for three different thicknesses (0.5, 0.75 and 1 cm).

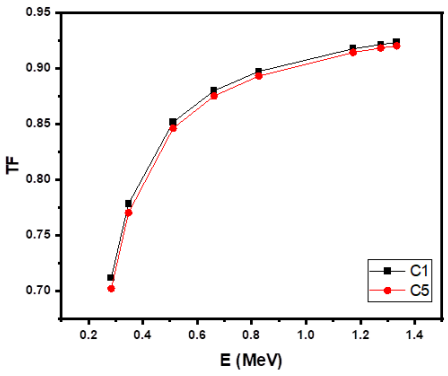

Figure 7. The transmission factor for C1 and C5 as a function of the energy.

interactions between the photons and the atoms will be occurred, so most of the photons are absorbed or scattered and can't penetrate the glass, leading to a small value of TVL. But the high energy radiation can easily penetrate the glass, so we need a thick sample to increase the interactions between the atoms of the glass and the photons, leading to high TVL at high energies.

In Fig. 6, we plotted the transmission factor (TF) for C1 only as a function of the energy for three different thicknesses (0.5, 0.75 and 1 cm). Two important points can be concluded from this figure. Firstly, the relation between the TF and the energy and secondly, the relation between the TF and the thickness of the glass [35]. For the first point, we observed a direct relation between the TF and the energy. As we mentioned in the previous paragraph, the high energy radiation can easily move through the medium and this is the reason for the increase in the TF with increasing the energy. This parameter gives information about the number of the photons that can move from the first side of the glass to another side, so if the TF for certain medium is high, then most of the photons can move thought the medium, while low TF indicates a good shielding performance of the medium. When we examined the relation between the TF and the thickness, we can see that the TF follows the order: $TF_{1cm} < TF_{0.75cm} < TF_{0.5cm}$. This confirms our finding in the TVL that the high thickness sample is more desirable in the radiation shielding applications [36].

In order to examine the impact of Cr_2O_3 on the shielding ability of the selected glasses, we plotted the TF for C1 and C5 in Fig. 7. At any energy, the TF for C1 is higher than that of C5, suggesting the adding more Cr_2O_3 to the glasses leads to decrease the number of photons that can penetrate the given glasses. So, the protection effectiveness of the glass with high Cr_2O_3 content is better than the glass with low Cr_2O_3 content.

4. Conclusion

We studied the radiation shielding parameters of Li_2O-Sb_2O_3-PbO-GeO_2-Cr_2O_3 glass systems at different energies ranging from 0.284 to 1.33 MeV. We investigated the impact of Cr_2O_3 on the radiation shielding parameters. The LAC showed an increase trend with the amount of Cr_2O_3, while the HVL showed a decrease trend with Cr_2O_3. The minimum HVL values were obtained at 0.284 MeV and varied between 0.98-1.02 cm. The HVL at 0.826 MeV is in the range of 3.072-3.201 cm, suggesting that it is important to increase the thickness of the glass to improve their shielding performance against high energy radiation. We investigated the TVL and an inverse relation is obtained between the TVL and the density of the glass. This HVL data showed that the impact of high energy radiation can be minimized by increasing the density of the glass sample. Also, the TVL data showed that the thickness increases by a factor of about 4 when the energy increases from 0.284 and 1.173 MeV.We examined the relation between the TF and the thickness, and the TF following order is reported: $TF_{1cm} < TF_{0.75cm} < TF_{0.5cm}$.

Ethical approval
This manuscript does not report on or involve the use of any animal or human data or tissue. So the ethical approval is not applicable.

Authors Contributions
Authors have equal contribution to prepare the paper. .

Availability of data and materials
The datasets used and/or analyzed during the current study available from the corresponding author.

Conflict of Interests
The authors declare that they have no known competing financial interests or personal relationships that could have appeared to influence the work reported in this paper.

References

[1] S. Hickling, L. Xiang, K. C. Jones, K. Parodi, W. Assmann, S. Avery, M. Hobson, and I. El. Naqa. "Ionizing radiation-induced acoustics for radiotherapy and diagnostic radiology applications.". *Medical Physics*, **45**: e707–e721, 2018.

[2] A. Sharma, M. I. Sayyed, O. Agar, and H. O. Tekin. "Simulation of shielding parameters for TeO_2-WO_3-GeO_2 glasses using FLUKA code.". *Results in Physics*, **13**:102199, 2019.

[3] Hassib. Mustafa Dh, Kawa M. Kaky, Ashok. Kumar, Erdem. Şakar, M. I. Sayyed, S. O. Baki, and M. A. Mahdi. "Boro-silicate glasses co-doped Er+ 3/Yb+ 3 for optical amplifier and gamma radiation shielding

applications". *Physica B: Condensed Matter*, **567**: 37–44, 2019.

[4] Alharshan. Gharam A, Canel. Eke, and M. S. Al-Buriahi. "Radiation-transmission and self-absorption factors of P2O5–SrO–Sb2O3 glass system". *Radiation Physics and Chemistry*, **193**:109938, 2022.

[5] S. A. M. Issa, A. Kumar, M.I. Sayyed, M.G. Dong, and Y. Elmahroug. "Mechanical and gamma-ray shielding properties of TeO_2-ZnO-NiO glasses.". *Materials Chemistry and Physics*, **212**:12–20, 2018.

[6] M. S. Al-Buriahi, Z. A. Alrowaili, S. J. Alsufyani, I. O. Olarinoye, A. N. Alharbi, C. Sriwunkum, and I. Kebaili. "The role of PbF_2 on the gamma-ray photon, charged particles, and neutron shielding prowess of novel lead fluoro bismuth borate glasses.". *Journal of Materials Science: Materials in Electronics 3*, **33**: 1123–1139, 2022.

[7] M. S. Al-Buriahi. "Radiation shielding performance of a borate-based glass system doped with bismuth oxide.)". *Radiation Physics and Chemistry*, **207**:110875, 2023.

[8] M. S. Al-Buriahi, D. K. Gaikwad, H. H. Hegazy, C. Sriwunkum, and R. Neffati. "Fe-based alloys and their shielding properties against directly and indirectly ionizing radiation by using FLUKA simulations.". *Physica Scripta*, **96**:045303, 2021.

[9] W. Keller and M. Modarres. "A historical overview of probabilistic risk assessment development and its use in the nuclear power industry: a tribute to the late Professor Norman Carl Rasmussen.". *Reliability Engineering & System Safety*, **89**:271–285, 2005.

[10] M. I. Sayyed, H. O. Tekin, O. Kılıcoglu, O. Agar, and M. H. M. Zaid. "Shielding features of concrete types containing sepiolite mineral: comprehensive study on experimental, XCOM and MCNPX results.". *Results in Physics*, **11**:40–45, 2018.

[11] I. Akkurt, H. Akyildirim, B. Mavi, S. Kilincarslan, and C. Basyigit. "Gamma-ray shielding properties of concrete including barite at different energies.". *Progress in Nuclear Energy*, **52**:620–623, 2010.

[12] M. I. Sayyed, K. A. Mahmoud, Sazirul. Islam, O. L. Tashlykov, E. Lacomme, and K. M. Kaky. "Application of the MCNP 5 code to simulate the shielding features of concrete samples with different aggregates.". *Radiation Physics and Chemistry*, **174**:108925, 2020.

[13] N. Nagaraja, H. C. Manjunatha, L. Seenappa, K. N. Sridhar, and H. B. Ramalingam. "Radiation shielding properties of silicon polymers.". *Radiation Physics and Chemistry*, **171**:108723, 2020.

[14] J. G. Scuderi, G. V. Brusovanik, D. R. Campbell, R. P. Henry, B. Kwon, and A. R. Vaccaro. "Evaluation of non–lead-based protective radiological material in spinal surgery.". *The Spine Journal*, **6**:577–582, 2006.

[15] S. J. B. Bin, K. S. Fong, B. W. Chua, and M. Gupta. "Mg-based bulk metallic glasses: A review of recent developments.". *Journal of Magnesium and Alloys*, **10**:899–914, 2022.

[16] J. Ding, C. Li, L. Zhu, D. Zhao, J. Li, and Y. Zhou. "$Pr_3Tm_3Er_3$ tri-doped tellurite glass with ultra-broadband luminescence in the optical communication band.". *Ceramics International*, **48**:8779–8782, 2022.

[17] E. Snoeks, G. N. van den Hoven, and A Polman. "Optimization of an Er-doped silica glass optical waveguide amplifier.". *IEEE Journal of Quantum Electronics*, **32**: 1680–1684, 1996.

[18] E. Williams and N. Lavery. "Laser processing of bulk metallic glass: A review.". *Journal of Materials Processing Technology*, **247**:73–91, 2017.

[19] P. R. Dias, L. Schmidt, N. L. Chang, M. M. Lunardi, R. Deng, B. Trigger, L. B. Gomes, R. Egan, and H. Veit. "High yield, low cost, environmentally friendly process to recycle silicon solar panels: Technical, economic and environmental feasibility assessment.". *Renewable and Sustainable Energy Reviews*, **169**:112900, 2022.

[20] H. E. Skallevold, D. Rokaya, Z. Khurshid, and M. S. Zafar. "Bioactive glass applications in dentistry.". *International Journal of Molecular Sciences*, **20**:5960, 2019.

[21] K. M. Kaky, G. Lakshminarayana, S. O. Baki, Y. H. Taufiq-Yap, I. V. Kityk, and M. A. Mahdi. "Structural, thermal, and optical analysis of zinc boro-aluminosilicate glasses containing different alkali and alkaline modifier ions.". *Journal of Non-Crystalline Solids*, **456**:55–63, 2017.

[22] A. AlRoos, N. Jamal, N. A. B. Amin, and R. Zainon. "Conventional and new lead-free radiation shielding materials for radiation protection in nuclear medicine: A review.". *Radiation Physics and Chemistry*, **165**: 108439, 2019.

[23] R. Vijay, P. R. Babu, V. R. Kumar, M. Piasecki, D. K. Rao, and N. Veeraiah. "Dielectric dispersion and ac conduction phenomena of Li_2O-Sb_2O_3-PbO-GeO_2: Cr_2O_3 glass system.". *Materials Science in Semiconductor Processing*, **35**:96–108, 2015.

[24] M. I. Sayyed. "Bismuth modified shielding properties of zinc boro-tellurite glasses.". *Journal of Alloys and Compounds*, **688**:111–117, 2016.

[25] C. Eke, O. Agar, C. Segebade, and I. Boztosun. "Attenuation properties of radiation shielding materials such as granite and marble against γ-ray energies between 80 and 1350 keV.". *Radiochimica Acta*, **105**:851–863, 2017.

[26] O. Agar, M. I. Sayyed, H. O. Tekin, K. M. Kaky, S. O. Baki, and I. Kityk. "An investigation on shielding properties of BaO, MoO_3 and P_2O_5 based glasses using MCNPX code.". *Results in Physics*, **12**:629–634, 2019.

[27] L. Gerward, N. Guilbert, K. Bjorn Jensen, and H. Levring. "WinXCom—a program for calculating X-ray attenuation coefficients.". *Radiation physics and chemistry*, **71**:653–654, 2004.

[28]

[29] A. Alalawi, M. S. Al-Buriahi, M. I. Sayyed, H. Akyildirim, H. Arslan, M. H. M. Zaid, and B. T. Tonguc. "Influence of lead and zinc oxides on the radiation shielding properties of tellurite glass systems.". *Ceramics International*, **46**:17300–17306, 2020.

[30] M. S. Al-Buriahi, C. Eke, Z. A. Alrowaili, A. M. Al-Baradi, I. Kebaili, and B. T. Tonguc. "Optical properties and radiation shielding performance of tellurite glasses containing Li_2O and MoO_3.". *OPTIK*, **249**: 168257, 2022.

[31] M. S. Al-Buriahi, D. K. Gaikwad, H. H. Hegazy, C. Sriwunkum, and H. Algarni. "Newly developed glasses containing Si/Cd/Li/Gd and their high performance for radiation applications: role of Er_2O_3.". *Journal of Materials Science: Materials in Electronics*, **32**:9440–9451, 2021.

[32] M. S. Al-Buriahi, I. O. Olarinoye, S. Alomairy, I. Kebaili, R. Kaya, H. Arslan, and B. T. Tonguc. "Dense and environment friendly bismuth barium tellurborate glasses for nuclear protection applications.". *Progress in Nuclear Energy*, **137**:103763, 2021.

[33] O. Agar., Z. Y. Khattari, M. I. Sayyed, H. O. Tekin, S. Al-Omari, M. Maghrabi, M. H. M. Zaid, and I. V. Kityk. "Evaluation of the shielding parameters of alkaline earth based phosphate glasses using MCNPX code.". *Results in Physics*, **12**:101–106, 2019.

[34] S. Kaewjaeng, N. Chanthima, J. Thongdang, S. Reungsri, S. Kothan, and J. Kaewkhao. "Synthesis and radiation properties of Li_2O-BaO-Bi_2O_3-P_2O_5 glasses.". *Materials Today: Proceedings*, **43**:2544–2553, 2021.

[35] K. A. Naseer, K. Marimuthu, K. A. Mahmoud, and M. I. Sayyed. "Impact of Bi_2O_3 modifier concentration on barium–zincborate glasses: physical, structural, elastic, and radiation-shielding properties.". *European Physical Journal Plus*, **136**:116, 2021.

[36] M. I. Sayyed, M. H. A. Mhareb, Y. S. M. Alajerami, K. A. Mahmoud, M. A. Imheidat, F. Alshahri, M. Alqahtani, and T. Al-Abdullah. "Optical and radiation shielding features for a new series of borate glass samples.". *OPTIK*, **239**:166790, 2021.